Self-organized phase segregation between inorganic nanocrystals and PC61BM for hybrid high-efficiency bulk heterojunction photovoltaic cells

Tsang, Sai-Wing; Fu, Huiying; Ouyang, Jianying; Zhang, Yanguang; Yu, Kui; Lu, Jianping

Publisher's version / Version de l'éditeur:
https://doi.org/10.1063/1.3454923
Applied Physics Letters, 96, 24, pp. 243104-1-243104-3, 2010-01-01

Self-organized phase segregation between inorganic nanocrystals and $PC_{61}BM$ for hybrid high-efficiency bulk heterojunction photovoltaic cells

Sai-Wing Tsang,[1] Huiying Fu,[1] Jianying Ouyang,[2] Yanguang Zhang,[1] Kui Yu,[2] Jianping Lu,[1,a)] and Ye Tao[1,a)]
[1]*Institute for Microstructural Sciences (IMS), National Research Council of Canada, Ottawa, Ontario K1A 0R6, Canada*
[2]*Steacie Institute for Molecular Sciences (SIMS), National Research Council of Canada, Ottawa, Ontario K1A 0R6, Canada*

(Received 18 March 2010; accepted 24 May 2010; published online 16 June 2010)

We demonstrate a simple approach to generate phase segregation between colloidal PbS nanocrystals (NCs) and organic [6,6]-phenyl C_{61} butyric acid methyl ester ($PC_{61}BM$). Continuous vertical phase segregation is observed in cross-linked composite films of NCs and $PC_{61}BM$. Hybrid bulk heterojunction photovoltaic cells fabricated with the phase segreated composite layer have achieved the state-of-art power conversion efficiency of 3.7% under one sun of simulated Air Mass 1.5 Global solar irradiation. The presented method can be generally applied in other NC/organic systems for the development of hybrid heterojunction photovoltaic cells. [doi:10.1063/1.3454923]

Photovoltaic (PV) cells based on solution processable colloidal nanocrystals (NCs) and organic semiconductors have drawn a lot of attention recently, owing to their low fabrication cost, large area capability, high optical absorbance, and the potential for high power conversion efficiency (PCE).[1,2] In addition, due to the quantum confinement effect, the optoelectronic properties of the NCs can be tuned by varying the size and shape of the NCs during the synthesis. Therefore, the optical absorption of NCs can cover a broader spectral range, from the visible to the infrared, offering optimal light absorption for PV applications. Due to the complementary optical absorption properties and the solution processability, NC/organic hybrid PV cells have attracted increasing research interests. However, most of such hybrid PV cells have PCEs of only around 2% or lower.[3] In most of those hybrid systems, the NCs are homogeneously dispersed in a polymer matrix. Due to the energy difference between the two materials and the absence of continuous phases of the NCs, at least one type of the charge carriers (electron or hole) is trapped inside the NCs with a long hopping distance to the adjacent NCs, which significantly reduces the photocurrent in the device. An efficient hybrid PV cell was demonstrated with an impressive PCE of 2.6% by using a blend of CdSe nanorods and poly(3-hexylthiophene) and a solvent with slow evaporation rate to enhance the self-organization of the polymer.[4] The approach is similar to the bulk heterojunction concept used in the polymer PV cells,[5,6] where the organic electron donor and acceptor materials form nanoscale interpenetrating networks which facilitate exciton dissociation and charge transport across the whole active layer. However, the lack of a continuous vertical distribution of the CdSe nanorods in the vertical direction makes it inefficient to extract the dissociated electrons from the system. It is well known that initiating and controlling the nanoscale phase segregation in a blend of electron donor and acceptor materials is a key to optimizing the device performance with solution processable PV materials.

In this work, a fast and simple method is demonstrated to develop hybrid bulk heterojunction PV cell with colloidal PbS NCs and organic [6,6]-phenyl C_{61} butyric acid methyl ester ($PC_{61}BM$). Phase segregation and continuous vertical phases of the PbS NCs and $PC_{61}BM$ are obtained by simply cross-linking the composite film at room temperature for a few minutes. The size of the segregated domains can be controlled with different weight (wt.) ratios between the PbS NCs and $PC_{61}BM$. As compared to the bilayer device fabricated from the same two materials, the bulk heterojunction approach has improved the PCE from 3.1% to 3.7%, which is attributed to the significant increase in the device's short circuit current (J_{SC}) from 7.61 to 10.01 mA/cm^2. Improved exciton dissociation in the bulk heterojunction device is evident from the internal quantum efficiency (IQE). We believe that this method can be generally applied to different colloidal NCs/organic systems and will facilitate the development of hybrid bulk heterojunction PV cells.

For the PV cell fabrication, indium tin oxide (ITO) coated glass was used as the anode. Immediately prior to device fabrication, the ITO glass was cleaned by ultrasonic baths of organic solvents (acetone and isopropanol) and then UV-ozone treated for 15 min. Oleic acid capped PbS NC (PbS-OA) solution in chloroform (5 mg/mL) was used to prepare the active layer. 1,3-benezendithiol (BDT) was used as the cross-linker to replace the OA surface ligand and bridge the NCs. Details about the NC synthesis, preparation of cross-linked PbS NC only films and device characterization are discussed in the supplementary materials.[7] For the bulk heterojunction devices, a solution of a mixture of PbS-OA NC and $PC_{61}BM$ in chloroform was spun (2500 rpm for 1 min) on top of a NC only layer to form a composite layer. The sample was then soaked in the cross-linker solution for 10 min to facilitate the phase segregation between the PbS NCs and the $PC_{61}BM$ molecules. It was followed by a spin-coating (2500 rpm, 1 min) the solution of $PC_{61}BM$ in chloroform (10 mg/mL) on top of the composite layer. Afterwards, the sample was transferred to an evaporation chamber without exposure to the air. Finally, 1 nm of LiF and 120 nm of Al were thermally evaporated on top of the

a)Authors to whom correspondence should be addressed. Electronic addresses: ye.tao@nrc-cnrc.gc.ca and jainping.lu@nrc-cnrc.gc.ca.

TABLE I. Summary of device structures used in this study. The devices have a general structure of ITO/PbS-BDT(40 nm)/composite layer (40 nm)/$PC_{61}BM$ (40 nm)/LiF (1 nm)/Al.

Device	Composite layer
A	PbS-BDT(40 nm)
B	PbS-BDT:$PC_{61}BM$(wt. ratio 50:1)
C	PbS-BDT:$PC_{61}BM$(wt. ratio 30:1)
D	PbS-BDT:$PC_{61}BM$(wt. ratio 10:1)

$PC_{61}BM$ to form the cathode. The PV cells had a general structure of ITO/active layer/LiF (1 nm)/Al (120 nm) with an active area of 9 mm^2. The device structures used in this study are summarized in Table I.

Figure 1 shows the atomic force microscopy (AFM) images of the cross-linked PbS NC only and composite films with different wt. ratios of PbS NCs and $PC_{61}BM$. Phase segregation of BDT linked PbS (PbS-BDT) NCs and $PC_{61}BM$ molecules in the cross-linked composite films have been observed. Figure 1 shows the surface morphologies of the cross-linked PbS-BDT only [Fig. 1(a)] and cross-linked PbS-BDT:$PC_{61}BM$ composite films prepared from solutions with PbS-OA:$PC_{61}BM$ wt. ratios of 50:1, 30:1, and 10:1 [Figs. 1(b)–1(d)], respectively. The films have similar surface roughness less than 3 nm. Szendrei *et al.* demonstrated that a mixture of PbS NCs capped with OA (PbS-OA) and $PC_{61}BM$ forms a homogeneous film without phase segregation.[8] Interestingly, as shown in the corresponding phase images [Figs. 1(e) and 1(h)] acquired *in situ* with the surface morphologies, segregated PbS-BDT (bright region) and $PC_{61}BM$ (dark region) domains are clearly present in our cross-linked composite films. During the cross-linking process, the OA surface ligands are replaced by the more reactive BDT cross-linker molecules. The two sulfur atoms in a BDT molecule can each form a strong bond with the surface Pb atoms of neighboring NCs and, therefore, bridge the NCs together. Since the size of BDT molecule is much smaller than that of OA, the cross-linking reaction can bring the NCs much closer and in the meanwhile expel $PC_{61}BM$ out of the NC domains. In addition, the sizes of PbS-BDT and $PC_{61}BM$ domain can also be controlled by using different wt. ratios of PbS-OA:$PC_{61}BM$. With increasing $PC_{61}BM$ content in the composite film, the $PC_{61}BM$ domains gradually emerge from the large PbS-BDT domains and eventually clusters of NCs

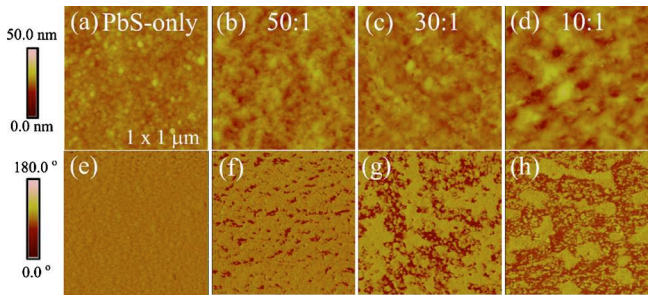

FIG. 1. (Color online) AFM images of the cross-linked PbS NC only and cross-linked composite films casted from solutions with different wt. ratios of PbS NCs and $PC_{61}BM$ molecules. The upper images (a), (b), (c), and (d) indicate the morphology of the cross-linked films prepared with PbS NC only and different wt. ratios of PbS-OA:$PC_{61}BM$ 50:1, 30:1, and 10:1 respectively. The lower images (e), (f), (g), and (h) which, respectively, corresponding to the morphology images (a), (b), (c), and (d), represent the *in situ* phase images. All images have the scan range of 1×1 μm^2.

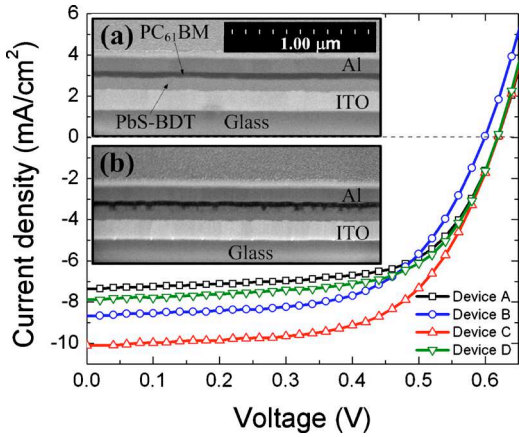

FIG. 2. (Color online) Measured current $J-V$ characteristics under one sun of simulated AM 1.5 G solar irradiation of the bilayer device A (black; square) and the bulk heterojunction devices B (blue; circle), C (red; up-triangle), and D (green; down-triangle) with different wt. ratios between PbS NCs and $PC_{61}BM$. Inset shows the cross-section SEM images of (a) the bilayer ITO/PbS-BDT/$PC_{61}BM$/LiF/Al device A and (b) the bulk heterojunction ITO/PbS-BDT/PbS-BDT:$PC_{61}BM$(wt. ratio 30:1)/$PC_{61}BM$/LiF/Al device C.

and $PC_{61}BM$ are formed. Such a phase segregated structure substantially increases the interfacial area between the two materials. In is worth noting that the small domains of $PC_{61}BM$ trapped in the NCs matrix, especially with wt. ratios 50:1 and 30:1, make the $PC_{61}BM$ difficult to be redissolved by the upper spin-coated layer, which is advantageous for preparing multilayer structures.

We fabricated hybrid bulk heterojunction PV cells with the cross-linked composite layer approach. With the same materials a bilayer device was also fabricated for comparison. The inset of Fig. 2 shows the cross-section scanning electron microscopy (SEM) images of bilayer device A [Fig. 2(a)] and bulk heterojunction device C [Fig. 2(b)]. For the bilayer heterojunction device, layers of PbS-BDT and $PC_{61}BM$ with an abrupt interface are clearly resolved between the ITO and Al electrodes. For the bulk heterojunction device, between the pure PbS-BDT and $PC_{61}BM$ layers, a cross-linked composite layer is observed, which contains interpenetrating networks of PbS-BDT and $PC_{61}BM$. Such bulk heterojunction device benefits from a few structural advantages as follows: larger contact area between the PbS-BDT and $PC_{61}BM$ domains increases the probability of exciton dissociation in both NCs and organics; the formation of interpenetrating donor and acceptor networks reduces the distance for the photogenerated excitons to diffuse to the heterojunction for dissociation; the composite film is sandwiched between two buffer layers of pristine PbS-BDT and $PC_{61}BM$, which suppresses the resistivity current under forward voltage bias; and more importantly, the continuous vertical phases of PbS-BDT and $PC_{61}BM$ in the composite film can facilitate the transport of the dissociated holes and electrons, respectively.

The PbS NCs used to fabricate the hybrid heterojunction devices are optimized with size and quality as discussed in the supplementary materials.[7] A NC only Schottky-type PV cell was fabricated with the same batch of NCs to evaluate the quality of the NCs. The device demonstrated a PCE of 3.2% under one sun of simulated Air Mass 1.5 Global (AM 1.5 G) solar irradiation. Figure 2 shows the current density–voltage ($J-V$) characteristics of the PbS-BDT/$PC_{61}BM$ bi-

TABLE II. Summary of the performance of bilayer and bulk heterojunction devices. The series resistances R_S of the devices are extracted at 1 V forward bias in dark condition.

Device	J_{SC} (EQE)[a] (mA/cm^2)	V_{OC} (V)	FF (%)	R_S (Ω cm^2)	PCE (EQE)[b] (%)
A	7.34 (7.61)	0.60	67	36.1	3.0 (3.1)
B	8.67 (8.86)	0.58	64	33.6	3.2 (3.3)
C	10.10 (10.01)	0.59	63	37.7	3.8 (3.7)
D	7.88 (8.46)	0.60	65	41.8	3.1 (3.3)

[a]The value insides the parentheses represent the calculated J_{SC} under 100 mW/cm^2 of AM 1.5 G solar illumination from the measured EQE data (wavelength: 300–1100 nm).
[b]The calibrated PCE with the calculated J_{SC} from the EQE data.

layer and the bulk heterojunction PV cells under one sun of simulated AM 1.5 G solar irradiation. Details of the PV cell structure and performances are summarized in Table I and Table II, respectively. Generally, the heterojunction devices have larger open circuit voltage (V_{OC}), 0.58–0.60 V, and fill-factor (FF), 63%–67%, than the NC only Schottky-type device (V_{OC}=0.56 V and FF=53%). It is attributed to the fact that the V_{OC} of a Schottky solar cell is limited to one half of its energy gap while the V_{OC} of a heterojunction device is not, and that the additional $PC_{61}BM$ layer that efficiently prevents excitons from quenching at the NC/metal interface, as reported in a similar system of PbS NC/C_{60} bilayer device.[9] As compared to the bilayer device A, the bulk heterojunction devices B–D have larger short circuit current (J_{SC}). The J_{SC} is increased from 7.34 mA/cm^2 in device A to 10.10 mA/cm^2 in device C. As a result, a maximum PCE of 3.7% has been achieved in the bulk heterojunction device with the optimal wt. ratio of 30:1 between PbS NCs and $PC_{61}BM$. Using the measured external quantum efficiency (EQE) data, we calculated the J_{SC} under 100 mW/cm^2 of AM 1.5 G solar irradiation as listed in Table II. The calculated values are consistent with the J_{SC} measured from the $J-V$ results, demonstrating negligible spectral mismatch in the PCE measurement. The increase in J_{SC} in the bulk heterojunction devices is attributed to the improved exciton dissociation with the interpenetrating networks of PbS NCs and $PC_{61}BM$ as discussed above. Moreover, the dependence of J_{SC} on the wt. ratios between the NCs and $PC_{61}BM$ also indicates that the exciton dissociation efficiency in the composite film is controlled by the domain size of the individual material. Such phenomenon is widely observed in polymer bulk heterojunction PV devices.[10,11] It is also worth noting that the series resistance R_S of the bulk heterojunction devices are similar to that of the bilayer device, neither the electron nor holes are trapped in the composite layer. It supports the argument of continuous vertical phase segregation as observed in the SEM measurement. The improved exciton dissociation efficiency in the bulk heterojunction devices is supported by the device quantum efficiency. As shown in Fig. 3, the measured EQE with a maximum of 40% in the bilayer device is increased to over 50% in the bulk heterojunction device. The IQEs [IQE=EQE/(1−R)] calculated using the EQE and device reflectance data are shown in the inset in Fig. 3. The IQEs of the bulk heterojunction devices have been increased in the whole spectral range. It further supports that the observed improvements in EQE and J_{SC} are

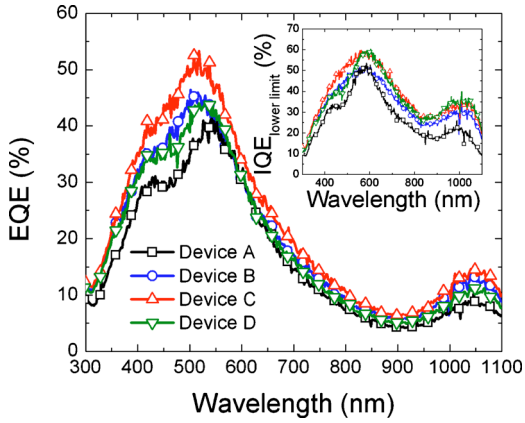

FIG. 3. (Color online) Measured EQEs spectra of the bilayer device A (black; square) and the bulk heterojunction devices B (blue; circle), C (red; up-triangle), and D (green; down-triangle) with different wt. ratios between PbS NCs and $PC_{61}BM$. Inset shows the estimated lower limit of the IQEs with the measured EQE and device reflectance data.

not due to the optical difference in the devices but because of the more efficient exciton dissociation in the bulk heterojunction structure.

In conclusion, cross-linking induced phase segregation in the composite thin film of PbS NCs and $PC_{61}BM$ has been demonstrated. The presented approach facilitates the fabrication of hybrid NC/organic bulk heterojunction PV cell with continuous phase segregation of individual material. The resulting solution-processed hybrid bulk heterojunction device has achieved a very promising PCE of 3.7% under one sun of simulated AM 1.5 G solar irradiation and improved EQE in a wide spectral range. The presented technique is expected to have wide applications in different NC/organic systems for the development of hybrid bulk heterojunction PV cells.

The authors would like to thank Hsien-Tse Tung, Dr. Xiaohua Wu, and Jeffrey W. Fraser for their experimental support. Valuable discussion on NC synthesis with Dr. Ruibing Wang is highly appreciated. The authors would also like to acknowledge the financial support from the National Research Council of Canada's NRC-Nano Initiative. H. Fu thanks the Chinese Scholarship Council for providing her PDF scholarship.

[1]G. Dennler, M. C. Scharber, T. Ameri, P. Denk, K. Forberich, C. Waldauf, and C. J. Brabec, Adv. Mater. (Weinheim, Ger.) **20**, 579 (2008).
[2]M. C. Hanna and A. J. Nozik, J. Appl. Phys. **100**, 074510 (2006).
[3]B. R. Saunders and M. L. Turner, Adv. Colloid Interface Sci. **138**, 1 (2008).
[4]B. Sun and N. C. Greenham, Phys. Chem. Chem. Phys. **8**, 3557 (2006).
[5]J. J. M. Halls, C. A. Walsh, N. C. Greenham, E. A. Marseglia, R. H. Friend, S. C. Moratti, and A. B. Holmes, Nature (London) **376**, 498 (1995).
[6]G. Yu, J. Gao, J. C. Hummelen, F. Wudl, and A. J. Heeger, Science **270**, 1789 (1995).
[7]See supplementary material at http://dx.doi.org/10.1063/1.3454923 for NC synthesis and device measurement and optimization.
[8]K. Szendrei, F. Cordella, M. V. Kovalenko, M. Böberl, G. Hesser, M. Yarema, D. Jarzab, O. V. Mikhnenko, A. Gocalinska, M. Saba, F. Quochi, A. Mura, G. Bongiovanni, P. W. M. Blom, W. Heiss, and M. A. Loi, Adv. Mater. (Weinheim, Ger.) **21**, 683 (2009).
[9]S. W. Tsang, H. Fu, R. Wang, J. Lu, K. Yu, and Y. Tao, Appl. Phys. Lett. **95**, 183505 (2009).
[10]W. Ma, C. Yang, X. Gong, K. Lee, and A. J. Heeger, Adv. Funct. Mater. **15**, 1617 (2005).
[11]G. Li, V. Shrotriya, J. Huang, Y. Yao, T. Moriarty, K. Emery, and Y. Yang, Nature Mater. **4**, 864 (2005).